

## Brief Reports

*Brief Reports are accounts of completed research which, while meeting the usual Physical Review standards of scientific quality, do not warrant regular articles. A Brief Report may be no longer than four printed pages and must be accompanied by an abstract. The same publication schedule as for regular articles is followed, and page proofs are sent to authors.*

### Percolation model for elastic softening in intermetallic compounds during solid-state amorphization

C. Massobrio

*Université Paris XI, Laboratoire des Composés Non-stoechiométriques, 91405 Orsay CEDEX, France*

V. Pontikis\*

*Centre d'Etudes de Saclay, Section de Recherches de Metallurgie Physique, 91191 Gif-sur-Yvette CEDEX, France*

(Received 1 May 1991)

By using isobaric-isothermal molecular dynamics and an  $n$ -body effective potential, we show that the amorphization of  $\text{NiZr}_2$ , mediated by chemical disorder, is preceded by an elastic softening and begins at the percolation threshold of the strain distortion regions associated with the antisite defects. The percolation model provides a unified description of the elastic softening and loss of crystalline order in intermetallic compounds resulting from irradiation or hydrogenation.

A considerable amount of experimental and theoretical results is now available to achieve a better understanding of solid-state reactions leading to the amorphization of intermetallic compounds.<sup>1</sup> The crystal line-to-amorphous ( $c$ - $a$ ) reaction is the response of a crystal to the structural and chemical disordering induced by an external perturbation, e.g., irradiation. Although the relative importance of Frenkel pairs and chemical disorder is still controversial,<sup>1-5</sup> the volume expansion and the softening of the elastic moduli that are observed during the amorphization process indicate that an elastic instability may be responsible for this behavior.<sup>1,6,7</sup> Moreover, experiments on  $\text{Zr}_3\text{Al}$  showed that the hydrogen-induced amorphization of this compound is produced at a lattice dilation identical to that found during irradiation.<sup>8</sup> Thus lattice expansion appears as a common measure of the crystal instability induced by different external perturbations and led to the suggestion that a thermodynamic parallel can be established between amorphization and melting. In an attempt to support this conjecture, Wolf *et al.*<sup>7</sup> showed recently that in the case of a Cu crystal the Born condition of elastic instability,  $2C' = C_{11} - C_{12} = 0$ , is satisfied when the isothermal volume expansion equals the critical value attained by heating isobarically the system up to mechanical melting. On the basis of these results it was suggested that solid-state amorphization processes, such as those brought about homogeneously and athermally by irradiation or hydrogen absorption, are driven by a mechanical instability much in the same way as melting.<sup>1,7</sup>

According to the model for the  $c$ - $a$  transition we present in the following, the elastic softening observed in intermetallic compounds under irradiation occurs at the percolation threshold of the strained regions surrounding the irradiation defects. Amorphization starts at the corresponding critical value of the long-range order param-

eter,  $S_c$ , but is completed much later. This model is supported by the behavior of the elastic moduli of crystalline  $\text{NiZr}_2$  computed by molecular dynamics (MD), while the system is chemically disordered. The motivation for selecting  $\text{NiZr}_2$  as a model system for this study is related to the existence of previous simulation work<sup>9,10</sup> which provided an  $n$ -body potential reproducing satisfactorily the properties of the real material. Since the implementation of the potential and the assessment of its reliability have been largely detailed in the literature<sup>9,10</sup> they will not be revised here. The computation of the elastic moduli is performed on a system made of 144 atoms (48 Ni and 96 Zr) in a  $2 \times 2 \times 3$  parallelepipedic box with periodic boundary conditions. A Gear fifth-order predictor-corrector algorithm with time step  $\Delta t = 10^{-15}$  s is employed throughout. Isothermal elastic constants for the crystal, the amorphous solid, and the chemically disordered system at zero stress are calculated in the  $(N\hbar T)$  ensemble, where  $\hbar$  is the matrix formed by the vectors  $\mathbf{a}$ ,  $\mathbf{b}$ , and  $\mathbf{c}$  which span the MD cell. The microscopic expression of the elastic constants to be averaged at equilibrium is the one detailed by Ray.<sup>11</sup> For each state point the zero stress condition for the crystal is achieved by using the variable size and shape extension of MD due to Parrinello and Rahman<sup>12</sup> and runs of up to  $10^5$  time steps. This provides the reference average values of  $\hbar$  to be used as input value in the  $(N\hbar T)$  calculations of elastic constants at the same temperature. Elastic moduli calculated for the amorphous solid, obtained by quenching the melt, are a useful reference to be compared with the values of the elastic constants of the disordered crystal at the transition threshold separating the crystalline from the amorphous behavior. The liquid state starting point of our cooling schedule and the configurations generated therefrom by quenching are first produced via the fixed shape form of constant pressure MD.<sup>13</sup> Then, for each

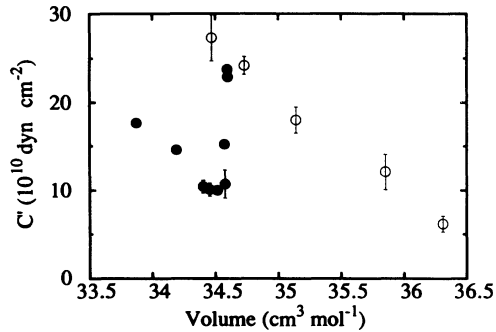


FIG. 1. Variation of the shear modulus of crystalline  $\text{NiZr}_2$  as a function of the molar volume. Solid circles: Data for values of the long-range order parameter ranging from  $S=1$  to 0.5. Open circles: Shear modulus of the amorphous solid obtained by quenching the liquid.

point in the amorphous region of the phase diagram thereby created, the elastic constants are calculated upon relaxation of the stress tensor to the desired zero value as indicated above. Typical error bars on each stress tensor component are of the order of 0.05 kbar. The system is kept at the desired temperature using the Nosé thermostat<sup>14</sup> in conjunction with either the Andersen<sup>13</sup> or the Parrinello-Rahman schemes.

Figure 1 displays the variation of the elastic modulus  $C' = (C_{11} - C_{12})/2$  as a function of the equilibrium molar volume of the crystal at  $T=300$  K for various levels of chemical disorder.  $C'$  corresponds to the eigenvalue of the elastic constant matrix,  $\underline{C}$ , closer to the boundary of the elastic instability condition defined by  $\det(\underline{C})=0$ . Average values of  $C'$  and the associated statistical errors are obtained by generating 10 statistically independent trajectories of  $10^5$  time steps each and are compared to those relative to the amorphous solid (Fig. 1, Table I).

For the latter, a single trajectory of  $10^5$  time steps has been used and the error bars are the deviation from the condition of isotropy inherent in a fully disordered system. The increasing disorder induces the simultaneous increase of the molar volume and the softening of the elastic modulus up to a dilation  $3\delta a/a \approx 2\%$ , which corresponds to a critical value of the long-range order parameter,  $S_c \approx 0.68$ , at which the  $c-a$  reaction is triggered. This behavior is qualitatively similar to the one exhibited by ion irradiated  $\text{Zr}_3\text{Al}$ .<sup>6</sup> For  $S \approx S_c$ , the shear modulus  $C'$  of the disordered solid increases suddenly up to a value comparable to the one we computed for the amorphous solid at the same molar volume (Fig. 1). Thus, the onset of the  $c-a$  transition is also reflected in the elastic properties of the model, as expected. The simulations reveal an interesting feature of the transition, namely its close resemblance to a second-order phase transformation. We notice that the error bars displayed in Fig. 1 are larger for the data lying around the molar volume corresponding to  $S_c$ , and this trend can be interpreted as the signature of an incoming phase transformation. It is legitimate to ask whether or not this behavior is related to a vanishing shear modulus  $C'$  in the neighborhood of  $S_c$ , thus corresponding to the occurrence of an elastic instability. Due to the small size of our system, only discrete  $S$  values can be explored and they are seen to lead systematically to nonzero values for the shear modulus  $C'$ . Therefore, in spite of the considerable decrease we found in the shear constant  $C'$  on increasing the chemical disorder, our results do not support the conjecture by Wolf *et al.*,<sup>7</sup> relating amorphization in its homogeneous mode to a mechanical instability. However, system size effects require a detailed investigation to decide whether the observed behavior may be consistent with the hypothesis of mechanical instability.

An indication which helped identifying the mechanism

TABLE I. Elastic constants of  $\text{NiZr}_2$  calculated upon introduction of an increasing number of antisite defects at  $T=300$  K (upper part) and for the amorphous solid produced by rapid quench at temperatures in the range  $300 \text{ K} \leq T \leq 1215 \text{ K}$  (lower part). The volume  $V$  is in units of  $\text{cm}^3/\text{mole}$  and the elastic constants  $C_{44}$ ,  $C_{55}$ ,  $C_{66}$ ,  $C'$ ,  $B$ , and  $G$  are in units of  $10^{10} \text{ dyne/cm}^2$ .  $B$  and  $G$  are the Voigt bulk and shear modulus averages, respectively;  $N$  is the length of the run in time steps ( $\Delta t = 10^{-15} \text{ s}$ ), and  $S$  the long-range order parameter.

$N$	$V$	$S$	$B$	$G$	$C'$	$C_{44}$	$C_{66}$
$10^6$	33.87	1	$109.5 \pm 1.1$	$34.3 \pm 0.5$	$17.6 \pm 0.4$	$44.3 \pm 0.3$	$42.1 \pm 1.1$
$10^6$	34.19	0.90	$108.0 \pm 1.1$	$30.8 \pm 0.5$	$14.6 \pm 0.4$	$38.5 \pm 0.3$	$40.0 \pm 1.1$
$10^6$	34.40	0.81	$104.9 \pm 1.0$	$25.4 \pm 0.5$	$10.4 \pm 0.7$	$35.2 \pm 0.3$	$33.2 \pm 0.5$
$10^6$	34.45	0.78	$104.5 \pm 1.0$	$24.5 \pm 0.5$	$10.1 \pm 0.7$	$30.2 \pm 0.3$	$31.1 \pm 0.5$
$10^6$	34.52	0.75	$104.3 \pm 1.0$	$26.0 \pm 0.5$	$10.0 \pm 0.3$	$33.9 \pm 0.3$	$32.0 \pm 0.2$
$10^6$	34.58	0.71	$103.3 \pm 1.0$	$19.9 \pm 0.6$	$10.7 \pm 1.6$	$23.6 \pm 1.3$	$21.5 \pm 2.2$
$10^6$	34.57	0.69	$103.3 \pm 1.0$	$23.1 \pm 0.5$	$15.2 \pm 0.4$	$25.6 \pm 0.3$	$26.7 \pm 1.1$
$10^6$	34.60	0.63	$104.2 \pm 1.0$	$23.5 \pm 0.5$	$22.9 \pm 0.4$	$22.7 \pm 0.3$	$25.7 \pm 1.1$
$10^6$	34.60	0.5	$103.6 \pm 1.0$	$24.0 \pm 0.5$	$23.8 \pm 0.4$	$26.6 \pm 0.3$	$23.7 \pm 1.1$
$N$	$V$	$T$ (K)	$B$	$G$	$C'$	$\frac{1}{3}(C_{44} + C_{55} + C_{66})$	
$10^5$	34.47	300	$103.5 \pm 9.5$	$23.4 \pm 2.6$	$27.3 \pm 2.6$	$22.2 \pm 2.6$	
$10^5$	34.73	460	$100.5 \pm 3.7$	$22.4 \pm 1.0$	$24.2 \pm 1.0$	$22.2 \pm 1.0$	
$10^5$	35.14	695	$93.3 \pm 5.5$	$16.1 \pm 1.5$	$18.0 \pm 1.5$	$15.1 \pm 1.5$	
$10^5$	35.85	930	$81.4 \pm 7.3$	$7.3 \pm 2.0$	$12.1 \pm 2.0$	$8.1 \pm 2.0$	
$10^5$	36.31	1215	$77.5 \pm 3.3$	$6.8 \pm 0.9$	$6.2 \pm 0.9$	$4.5 \pm 0.9$	

responsible for the  $c$ - $a$  transition is provided by the analysis of the distortions generated by the antisite defects. To this purpose, a single antisite defect has been introduced into the system and the lowest-energy configuration has been obtained by energy minimization. Large nonelastic relaxations of the matrix, reaching values up to 13% at a second-neighbor distance, take place around the exchanged atoms. This observation suggests that the large variation of  $C'$  in the vicinity of  $S_c$  and the onset of the  $c$ - $a$  transformation may be related to the percolation of the distorted regions around antisite defects. To test the percolation hypothesis we analyzed the Voigt elastic moduli  $G$  and  $B$  of the crystal<sup>15</sup> in terms of the probability of finding a Ni atom on a site pertaining to the nickel sublattice and we performed a power-law fit, of the kind  $G$  and  $B \approx (S - S_c)^\alpha$ , in the region  $S > S_c$ . Exponents  $\alpha_G = 1.23$  and  $\alpha_B = 1.39$  are respectively obtained and the value  $S_c = 0.688$  is thereby determined, in good agreement with our previous more empirical determination  $S_c \approx 0.6$ .<sup>9,10</sup> To give confidence to the idea that the  $c$ - $a$  transformation begins when the critical volume fraction of the disordered material reaches the three-dimensional (3D) percolation threshold, the value of the effective volume increase per antisite defect is needed. This quantity has been extracted from our simulations as follows: At low levels of disorder (high  $S$  values), antisite defects should behave as dissolved impurities and the elastic model of dilute solid solutions<sup>16,17</sup> can be applied. Accordingly, the elastic energy stored into this "solid solution" is given by  $E_{el} = W_0 c(1 - c)$ , where  $W_0$  is the elastic energy increase per impurity (in the present case per antisite defect) and  $c$  the volume fraction of impurities. The latter is given by

$$c = \frac{n_d v_d}{N_T v_0} = \frac{2}{3} (1 - S) \frac{v_d}{v_0}, \quad (1)$$

where  $n_d$ ,  $N_T$ ,  $v_d$ , and  $v_0$  represent, respectively, the number of antisite defects, the total number of molecules contained into the system, the effective molar volume of an antisite defect, and the one associated with the perfect crystal. Figure 2 represents the variation of the excess energy of our model system as a function of  $1 - S$  and the dashed line corresponds to the fit of the elastic model prediction to the MD data. A least-squares minimization

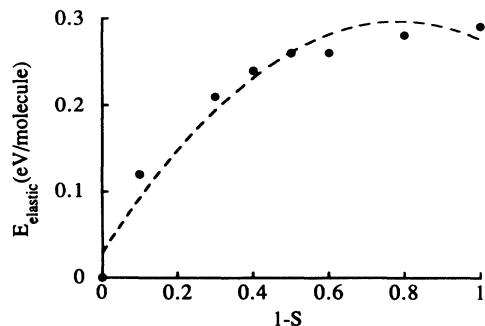


FIG. 2. Excess energy stored into the system as a function of  $1 - S$ , proportional to the number of antisite defects. The dashed line is a fit of the elastic model of solid solution to the MD data.

leads to the values  $W_0 = 0.92$  eV/molecule and  $x = v_d/v_0 = 1.139$ . By using this value of  $x$  and the above determined  $S_c = 0.688$ , the volume fraction corresponding to the threshold for 3D percolation of the distorted regions surrounding the antisite defects takes the value  $c \approx 0.24$ . This value is close to the theoretically predicted critical volume fraction for percolation of impermeable spheres on a rigid lattice,  $\phi_c = 0.15$ .<sup>18</sup> It is worth noting that the percolation scheme provides a common representation of the simultaneous elastic softening of the shear and bulk moduli of the disordered crystal, as opposed to models attributing a key role to dilation.<sup>16,17</sup> In addition, we point out that the static structure factor computed for several values of the wave vector shows clearly that certain crystalline features persist for values of  $S$  well below  $S_c$ . This can be seen from Fig. 3 and proves that amorphization is completed only for values of  $S < S_c$ , much closer to the experimental result obtained for  $Zr_3Al$ ,  $S \approx 0.2$ .<sup>6</sup> This result is consistent with experimental evidence and confirms that amorphization is completed at a much later irradiation stage than the one at which the onset of a local transformation is resolved experimentally.

Although the percolation hypothesis needs extensive experimental validation, it is of interest to examine its possible implications on the experimental side. Depending on the nature of the alloy under consideration, amorphization may be driven by Frenkel pairs and not by antisite defects as indicated by computer simulation studies of the amorphization in Cu-Ti (Ref. 2) and Ni-Ti (Ref. 3) alloys. On the other hand, whenever the total volume fraction of the strained regions associated with the active defect exceeds the critical value for percolation, elastic softening is expected to originate either high-energy metastable states<sup>3</sup> or fully amorphous structures.<sup>9,10</sup> Accordingly, the kind of disorder controlling the possible occurrence of the  $c$ - $a$  transition depends on the relative facility of creating by irradiation antisite defects or interstitials, on the kinetics of recombination of Frenkel pairs, and on the relative importance of the strain distortions around the defects. Moreover, the percolation hypothesis provides a unifying basis for amorphization by irradiation or hydrogenation. The suggestion by Okamoto

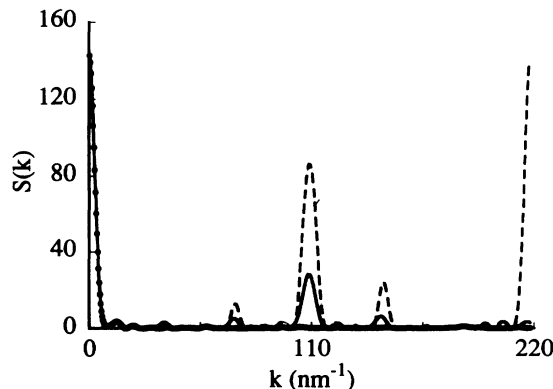


FIG. 3. Total static structure factor as a function of the wave vector,  $k_{\parallel[111]}$ , computed for several values of the long-range order parameter  $S$ , dashed line:  $S = 1$ , solid line  $S = 0.5$ , open circles (thick solid line)  $S = 0$ .

*et al.*,<sup>1</sup> considering dilation as the common factor between these processes, is consistent with the present approach for which the relevant quantity is the amount of distortion introduced in the lattice by hydrogen or antisite defects. As a natural consequence of the percolation scheme, the threshold for the *c-a* reaction may never be reached in binary alloys,  $A_xB_y$ , for low values of *x* or *y*. Therefore it should exist a domain of compositions such that even a lattice fully chemically disordered cannot become amorphous. On the basis of our results for

NiZr<sub>2</sub>, these composition limits, expressed in Ni content, are respectively 19% and 81%. Work is now in progress in order to further test the percolation model and its consistency with experiments.

We wish to thank J. L. Bocquet and G. Martin for useful discussions. Laboratoire de Composés Non-stoechiométriques is Unité Associée No. 446 du Centre National de la Recherche Scientifique.

---

\*To whom correspondence should be addressed.

<sup>1</sup>P. R. Okamoto and M. Meshii, ASM Materials Science Seminar, Chicago, IL, 1988, in *Science of Advanced Materials*, edited by H. Wiedersich and M. Meshii (ASM International, Ohio, 1990).

<sup>2</sup>M. J. Sabochick and N. Q. Lam, *Phys. Rev. B* **43**, 5243 (1991).

<sup>3</sup>M. J. Sabochick and N. Q. Lam, Materials Research Society Proceedings, Symposium F: Kinetics of Phase Transformations, Boston, MA, 1990 (unpublished).

<sup>4</sup>Y. Limoge, A. Rahman, H. Hsieh, and S. Yip, *J. Non-Cryst. Solids* **99**, 75 (1988).

<sup>5</sup>H. Hsieh and S. Yip, *Phys. Rev. B* **39**, 7476 (1989).

<sup>6</sup>L. E. Rehn, P. R. Okamoto, J. Pearson, R. Bhadra, and M. Grimsditch, *Phys. Rev. Lett.* **59**, 2987 (1987).

<sup>7</sup>D. Wolf, P. R. Okamoto, S. Yip, J. F. Lutsko, and M. Kluge, *J. Mater. Res.* **5**, 286 (1990).

<sup>8</sup>W. J. Meng, J. Faber, Jr., P. R. Okamoto, L. E. Rehn, B. J. Kestel, and R. L. Hitterman, *J. Appl. Phys.* **67**, 1312 (1990).

<sup>9</sup>C. Massobrio, V. Pontikis, and G. Martin, *Phys. Rev. Lett.* **62**, 1142 (1989).

<sup>10</sup>C. Massobrio, V. Pontikis, and G. Martin, *Phys. Rev. B* **41**, 10486 (1990).

<sup>11</sup>J. Ray, *Comput. Phys. Commun.* **8**, 109 (1988).

<sup>12</sup>M. Parrinello and A. Rahman, *J. Appl. Phys.* **52**, 7182 (1981).

<sup>13</sup>H. C. Andersen, *J. Chem. Phys.* **72**, 2384 (1980).

<sup>14</sup>S. Nosé, *J. Chem. Phys.* **81**, 511 (1984).

<sup>15</sup>D. J. Oh and R. A. Johnson, *J. Mater. Res.* **3**, 471 (1988).

<sup>16</sup>J. Friedel, *Philos. Mag.* **46**, 514 (1955).

<sup>17</sup>J. D. Eshelby, in *Solid State Physics*, edited by F. Seitz and D. Turnbull (Academic, New York, 1956), Vol. 3, p. 79.

<sup>18</sup>I. Balberg, *Philos. Mag. B* **56**, 991 (1987).